



HAL
open science

Process-based analysis of *Thinopyrum intermedium* phenological development highlights the importance of dual induction for reproductive growth and agronomic performance

Olivier Duchene, Benjamin Dumont, Douglas J Cattani, Laura Fagnant, Brandon Schlautman, Lee R Dehaan, Spencer Barriball, Jacob M Jungers, Valentin D Picasso, Christophe David, et al.

► To cite this version:

Olivier Duchene, Benjamin Dumont, Douglas J Cattani, Laura Fagnant, Brandon Schlautman, et al.. Process-based analysis of *Thinopyrum intermedium* phenological development highlights the importance of dual induction for reproductive growth and agronomic performance. *Agricultural and Forest Meteorology*, 2021, 301-302, pp.108341. 10.1016/j.agrformet.2021.108341 . hal-03185081

HAL Id: hal-03185081

<https://hal.science/hal-03185081>

Submitted on 22 Nov 2021

HAL is a multi-disciplinary open access archive for the deposit and dissemination of scientific research documents, whether they are published or not. The documents may come from teaching and research institutions in France or abroad, or from public or private research centers.

L'archive ouverte pluridisciplinaire **HAL**, est destinée au dépôt et à la diffusion de documents scientifiques de niveau recherche, publiés ou non, émanant des établissements d'enseignement et de recherche français ou étrangers, des laboratoires publics ou privés.

1 Process-based analysis of *Thinopyrum intermedium* phenological development
2 highlights the importance of dual induction for reproductive growth and agronomic
3 performance

4

5 Olivier Duchene*^{1§}, Benjamin Dumont^{2§}, Douglas J. Cattani³, Laura Fagnant², Brandon Schlautman⁴,
6 Lee R. DeHaan⁴, Spencer Barriball⁴, Jacob M. Jungers⁵, Valentin D. Picasso⁶, Christophe David¹, Florian
7 Celette¹

8 [§] **The authors contributed equally to the paper**

9 ***corresponding author:** olduchene@isara.fr; +33631460196

10 ¹ ISARA, Agroecology and Environment Research Unit, 23 Rue Jean Baldassini, 69364, Lyon cedex 07, France

11 ² ULiege - Gembloux AgroBio-Tech, Plant Sciences Axis, Crop Science lab., B- 5030 Gembloux, Belgium

12 ³ Department of Plant Science, University of Manitoba, 66 Dafoe Road, Winnipeg, Manitoba, Canada R3T 2N2.

13 ⁴ The Land Institute, 2440 E. Water Well Rd., Salina, KS, 67401, USA

14 ⁵ Department of Agronomy and Plant Genetics, University of Minnesota, St. Paul, MN 55108, USA

15 ⁶ Department of Agronomy, University of Wisconsin – Madison, 1575 Linden Dr., Madison, WI, 53706, USA

16 **Keywords**

17 *Thinopyrum intermedium*; perennial grains; flowering induction; photoperiod; modelling

18 **Highlights**

- 19
- IWG reproductive growth requires a vernalization treatment
- 20
- In spring, IWG reproductive growth is associated with GDD accumulation and photoperiodic
- 21 response
- 22
- GDD-daylength coupled dynamics drive IWG sward functional changes during reproductive
- 23 growth
- 24
- GDD-daylength coupled dynamics can inform and improve agronomic management.

25 Abstract

26 Intermediate wheatgrass (*Thinopyrum intermedium* (Host) Barkworth & D.R. Dewey) is being
27 developed for use as a new perennial grain crop through breeding and agronomic research.
28 However, progress has been hampered by lack of understanding of environmental requirements for
29 flowering and grain production. Therefore, we developed a phenology model for IWG adapted from
30 the STICS soil-crop model. The model was compliant with experimental results (relative root mean
31 square error = 0.03). The optimal vernalizing temperature was between 4 and 5°C, optimal daylength
32 between 13 and 14h, while daylength below 11h slowed reproductive development. Vernalization
33 requirement was found to be a constraining inductive process. Including a photoperiod limitation to
34 the model with temperature improved its ability to predict induction at various latitudes. Therefore,
35 timing and duration of vegetative vs. reproductive growth may differ between environments and
36 change reproductive tiller elongation earliness, weed competitiveness, management timing, and
37 stress conditions during phases critical to grain yield. Accurate phenology models will enable optimal
38 field management and inform future breeding strategies. However, plasticity may lead to divergent
39 ideotypes under various agroecosystems.

40 1. Introduction

41 The wheat-relative intermediate wheatgrass (*Thinopyrum intermedium* (Host) Barkworth & D.R.
42 Dewey) (IWG) is a winter-hardy cool-season perennial grass, which has recently undergone
43 development as a perennial grain by several breeding programs (Bajgain et al., 2020). Improved IWG
44 populations have been released by *The Land Institute* (Salina, Kansas, USA) under the trade name
45 Kernza® (DeHaan et al., 2018). Intermediate wheatgrass can support the transition to agroecological
46 systems because this perennial crop produces forage and grain for several years with minimal soil
47 disturbance and associated environmental issues (Duchene et al., 2019; Ryan et al., 2018). Featuring
48 large and deep roots, year-round soil cover, increased resource use efficiency and an extended
49 growing season (Cattani and Asselin, 2018a; DeHaan, 2015; Glover et al., 2010; Sprunger et al., 2018),

50 the 'perennialization' of cropping systems would be one cornerstone of sustainable agriculture
51 (Crews, 2016).

52

53 Intermediate wheatgrass has relatively low grain yields compared with annual cereal grains (Jungers
54 et al., 2018, 2017; Tautges et al., 2018), which has limited the introduction and adoption of IWG into
55 grain systems and crop rotations. Seed production is the result of the interaction between genotype
56 and growth conditions. Breeding efforts have been mostly dedicated to improving shatter resistance
57 and free-threshing seeds, along with larger seed mass and seed number per head (DeHaan et al.,
58 2018). Little attention has been paid to IWG phenological milestones that determine its growth cycle
59 (inductive transition), from the initiation of inflorescence primordia to seed maturity. Current
60 worldwide endeavors and interest in IWG production is driving the need for deeper investigation of
61 the environmental requirements associated with IWG yield and yield components. Filling this
62 knowledge gap would provide direction in targeting specific breeding strategies, suitable growing
63 contexts, and best crop management practices to optimize IWG grain production.

64

65 Winter annual herbaceous grains, like winter wheat, and most perennial grasses have a dual
66 induction requirement for flowering (Cooper and Calder, 1964; Heide, 1994). The primary induction
67 includes exposure to winter conditions, including low temperatures (LT) and short daylength (SD),
68 which is followed by a secondary induction that includes a period of transition to longer days (LD)
69 and higher temperatures (HT; Heide, 1994). Primary induction is usually discussed as the
70 vernalization process, corresponding to a chilling treatment that induce reproductive primordia
71 (Seppänen et al., 2013). Cold resistance is gradually improved through low-temperature acclimation,
72 and then gradually lost with time, cooler temperatures and vernalization saturation (Fowler et al.,
73 1996; Limin and Fowler, 2006). The secondary induction follows as a critical accumulation of heat
74 units (growing degree-day) and increased daylengths that stimulate a crop's phasic development,
75 tiller growth and flowering (Basu et al., 2012; Chouard, 1960; Trione and Metzger, 1970).

76

77 In winter grain crops and forage grasses, the achievement of primary induction (vernalization) needs
78 either LT or SD, but sometimes requires both (e.g. *Bromus inermis*), or has a preferential
79 temperature/photoperiod inductive pathway (e.g. *Phleum nodosum*, *Agrostis canina*; Cooper and
80 Calder, 1964; Halevy, 1989). Temperature and photoperiod are interactive factors since a change in
81 one parameter can modify inductive requirements of the other (Halevy, 1989; Heide, 1994; Limin and
82 Fowler, 2006; Mahfoozi et al., 2000; Ritchie, 1991). However, warm-season perennial grasses (e.g.
83 *Panicum virgatum*, *Andropogon gerardii*), and certain cool-season species (e.g. *Phleum pratense*) do
84 not require vernalization to achieve flowering (Table S1). Moreover, population diversity, breeding,
85 and plant life-history in fields leads to a certain variability or heterogeneity of inductive requirements
86 among the same species, with the potential formation of cultivars or local ecotypes (Dubcovsky et al.,
87 2006 Cooper and Calder, 1964; Jokela et al., 2015; Palit et al., 2014). Considering IWG, the need of
88 primary induction (vernalization treatment) to ensure proper reproductive growth has been shown
89 previously (Frischknecht, 1959) and has been recently confirmed by field observations and results
90 from controlled experiments (Ivancic et al, *under review*).

91

92 The transition from winter dormancy to spring growth and flowering (secondary induction) vary
93 greatly among perennial grasses in terms of timing and environmental requirements (Ansquer et al.,
94 2009). Flowering earliness generally differentiates fast growing species with generally lower
95 requirements. Conversely, late maturing species generally require greater heat unit accumulation,
96 associated with higher phyllochrons, to achieve flowering (Duru et al., 1993, 2008b; Frank and Bauer,
97 1995). Photoperiod mediation of the growth period is observable in many species, with different
98 degrees of importance, late flowering and single induction grasses would depend solely on
99 photoperiod responsiveness (Castro et al., 2011; Esbroeck et al., 2003; Mitchell et al., 1997).
100 Considering IWG, the role of photoperiod in reproductive growth has been suggested before and

101 would have been a driver of later tiller elongation as compared to other perennial grasses such as
102 *Bromus inermis* (Mitchell et al., 1998).

103

104 Linking plant phenology to whole plant growth and resource use strategy, fast or slow growing
105 patterns of forage grasses appears to be associated with several functional traits (e.g. organ turnover
106 rate, specific leaf area, biomass density, leaf nitrogen concentration, net primary productivity; Cruz
107 et al., 2010; Duru et al., 2008, 2009; Ryser and Lambers, 1995; Shipley, 2006) which, when combined,
108 determine the resource-conservative or acquisitive growth strategies of these grass species in their
109 native ecosystems.

110

111 This study used a large pool of phenological field observations from various regions and across
112 different cropping seasons to evaluate IWG phasic development *in situ*. To complement other studies
113 designed in controlled conditions (Ivancic et al., *under review*), this dataset offers an unprecedented
114 opportunity to look at the influence of divergent temperature and daylength conditions on IWG
115 growth. The use of integrative crop modelling concepts is then a powerful way to provide a more
116 holistic understanding of the crop growth dynamic within a specific environment. Coupling field
117 observations and modeling approaches notably enables the analysis of complex biotic and abiotic
118 interactions through the integration of growth function and process-based data.

119

120 The objective was to accurately characterize the converging drivers of phenological development of
121 IWG populations in diverse growth environments. In particular, three questions were addressed: i)
122 How sensitive is IWG to vernalization and what are its vernalization requirements?; ii) How sensitive
123 is IWG to photoperiod during secondary induction and what are the photoperiod thresholds of IWG?;
124 and iii) How fast does IWG develop in various agronomic conditions? These questions were examined
125 through field-based measurement analysis and crop model inversion of IWG phenological
126 development. IWG phenology and environmental requirements are discussed and compared to the

127 existing literature on perennial grasses and annual winter grain crops, with the purpose to better
128 place IWG growth among already characterized functional groups. Overall, this work aims to evaluate
129 opportunities and challenges in terms of adequacy and integration of IWG as a perennial grain into
130 farming systems.

131

132 2. Materials and methods

133 To characterize IWG phenological responses to contrasted growing environments, and compare its
134 behavior to known perennial grasses or annual grain crops characterized in the literature (section
135 2.1), a database was constructed with experiments conducted across Western Europe and North
136 America (section 2.2). In an attempt to better understand crop response to those conditions, field
137 result analysis was coupled with crop modeling approaches. Classic field result analysis, consisting of
138 comparing phenological stages and degree-day accumulation starting February 01 (shown to
139 minimize GDD accumulation variability and corresponding to plant changes in assimilate allocation;
140 Ansquer et al., 2009; Peacock, 1976), was first conducted (section 2.3). Crop modeling approaches
141 were then deployed to further ascertain the impacts of vernalization and photoperiod on the
142 phenological development (section 2.4).

143 **2.1. Experimental sites and data collection**

144 [2.1.1. Site description and experimental conditions](#)

145 From 2012 to 2019, IWG field experiments were conducted in four countries (USA, Canada, France
146 and Belgium). Data were thus respectively collected under Köppen climate (Peel et al., 2007) type
147 Dfb in Canada (humid continental climate conditions), type Dfa in the USA (hot summer continental
148 climate conditions) and type Cfb in France and Belgium (temperate climatic conditions characterized
149 by warm summers). These climatic contexts allowed evaluation of various temperature patterns and
150 seasonal conditions to assess the accumulation of heat units and vernalization requirements.

151 Furthermore, latitudes of the different sites ranged between 38.77°N and 50.56°N (Table S2)
152 inducing contrasted photoperiods.

153 2.1.2. Data collection

154 For each location, precipitation and average temperatures were measured daily. IWG growth stages
155 were measured at the field level, representing the dominant growth stage of the stand, and were
156 rated using the BBCH scale (Hess et al., 1997) and the timing of each observation was reported in
157 DAE/DAH unit (day after emergence/ day after last harvest). In this paper the focus was put on four
158 main phenological stages:

- 159 ▪ stem elongation (BBCH 30), which characterize the end the juvenile phase and the beginning
160 of shoot development;
- 161 ▪ flag leaf (BBCH 39) accounts for the end of foliar development;
- 162 ▪ flowering (anthesis) (BBCH 65) represents the end of shoot development and the beginning
163 of grain filling;
- 164 ▪ maturity (BBCH 89), which stands for the end of grain filling and the cessation of the
165 reproductive cycle.

166 A total of 137 phenological observations were recorded on these main phenological stages.

167

168 2.2. Growing-degree-day calculation

169 Following the approach of Ansquer et al. (2009), growing-degree-day (GDD) in base 0 was computed
170 as:

171

$$172 \quad T_{mean}(i) = \frac{T_{max}(i) - T_{min}(i)}{2} \quad \text{Eq. 1}$$

$$173 \quad GDD(i) = T_{mean}(i) - T_{base} \quad \text{Eq. 2}$$

174

175 In which i is a given day, T_{max} , T_{min} and T_{mean} are respectively the maximal, minimal and mean air
176 temperature recorded for day i and T_{base} is the base temperature (assumed to be 0 in this case).

177 As in Ansquer et al. (2009), and as usually done for perennial crops, the sum of GDD is usually
178 computed starting Feb. 01 in France. In this paper, the sum of GDD was computed from February, 01
179 and accumulated up to flowering (BBCH 65). This approach has demonstrated its relevance to
180 determine grass development milestones (Ansquer et al. 2009 ; Bartholomew and Williams, 2005 ;
181 Brown et al., 1986 ; Chauvel et al., 2000 ; Frank and Hofmann, 1989 ; Mitchell et al., 1997). Using a
182 constant base temperature over which any additional degree is accumulated as a temperature
183 enabling developmental unit is largely used (e.g. Ansquer et al., 2004 ; Cruz et al., 2010 ; Duru et al.,
184 2008c ; Luo et al. 2011 ; Parthasarathi et al., 2013). Such an approach has been integrated in most
185 plant growth models (Wang et al., 2017).

186

187 **2.3. Crop modelling**

188 The crop model approach deployed in this paper adopts the formalisms used in the widely validated
189 STICS soil-crop model (Brisson et al., 2009, 2002, 1998). We propose here a short description of the
190 different formalisms. Further details are found in Brisson et al. (2009).

191 **2.3.1. Phenological development**

192 As for many crop models, the simulation of succession of different phenological stages is driven by
193 the accumulation of “*development units*”. To compute these, we kept from the STICS model the
194 impacts of temperature, photoperiod and cold requirements, while we set aside the slowing impacts
195 of water and nitrogen stress. The *development units* considered here are computed at the daily time
196 step as follows:

197

$$198 \quad UPVT(i) = GDD_t(i) \cdot SFP(i) \cdot SFV(i) \quad \text{Eq. 3}$$

199

200 In which i is the considered day, $UPVT$ are Photo-Vernalo-Thermic Units ($UPVT$ in short), GDD_t are the
201 growing degrees-days limited by thresholds, SFP is a Slowdown Factor accounting for Photoperiod,
202 and SFV is a Slowdown Factor accounting for Vernalization.

203 Under this formalization, the accumulation of development units is firstly driven by the widely-
 204 accepted concept of growing degrees-days (Durand, 1967). Comparing to the simple Eq. 2, the
 205 concept of growing degree-day used here (GDD_t) is adapted to account for minimal, optimal and
 206 maximal temperature thresholds (Eq. 4). Photoperiod (Eq.5) and cold requirement (Eq.6) are used to
 207 slow down the accumulation of development units; as suggested by Brisson and Delecolle (1992),
 208 these effects are computed as a rate applied per unit of thermal time, implying the use of
 209 multiplicative terms in eq.3.

210 Finally, the last step of phenological development simulation was to sum UPVT over the cropping
 211 season. To do so, UPVT were summed starting from the day of emergence (establishment year) or
 212 the day following previous harvest (other years) up to the harvest of the considered crop season.
 213 Regarding the simulation of one particular stage (BBCH 30, 39, 65 or 89 – see section “Data
 214 collection”), the model calibration involved retrieving the sum of UPVT that was required to reach a
 215 specific stage while optimizing the model performances (see section “Assessment of model
 216 performance”).

217 2.3.2. Effect of temperature

218 The impacts of temperature respond to a triangular function (Eq.4)

219

$$\left\{ \begin{array}{ll} GDD_t(i) = 0 & \text{if } T_{mean}(i) \leq DT_{min} \text{ or } T_{mean}(i) \geq DT_{max} \\ GDD_t(i) = T_{mean}(i) - DT_{min} & \text{if } DT_{min} < T_{mean}(i) \leq DT_{opt} \\ GDD_t(i) = \frac{DT_{opt} - DT_{min}}{DT_{opt} - DT_{max}} \cdot (T_{mean}(i) - DT_{max}) & \text{if } DT_{opt} < T_{mean}(i) < DT_{max} \end{array} \right.$$

220 **Eq. 4**

221

222 In which DT_{min} , DT_{opt} and DT_{max} are the minimal, optimal and maximal temperature to allow for crop
 223 development. In particular, here, DT_{min} is the equivalent of T_{base} proposed at equation 2.

224 Under such conditions, the effects of temperature on crop development are linearly increasing
 225 between DT_{min} and DT_{opt} and are linearly decreasing between DT_{opt} and DT_{max} . DT_{opt} and DT_{max} have

226 been proposed in Brisson et al. (2008) to account for the slowdown in crop development that can be
227 observed under hot conditions.

228 2.3.3. Photoperiod factor

229 Using classic astronomical functions, the photoperiod (PhotoP(i) in Eq.5) can be calculated on the
230 basis of the calendar days and the latitude (Sellers, 1965). Based on the photoperiod, the slow-down
231 photoperiodic effect SFP(i) can then be calculated using Eq. 5.

232

$$233 \begin{cases} SFP(i) = \frac{(PhotoP(i) - PhotoP_{sat})}{(PhotoP_{sat} - PhotoP_{base})} + 1 \\ SFP(i) = \max(\min(SFP(i), 1), 0) \end{cases} \quad \text{Eq. 5}$$

234

235 In which PhotoP_{base} is the photoperiod below which there is no development and PhotoP_{sat} is the
236 saturation photoperiod, above which there is no limitation. The second term of Eq.5 ensures that
237 SFP(i) is mathematically bounded between 0 and 1.

238

239 We assumed that IWG would be a long-day plant (Heide, 1994) similar to other grassland species and
240 most annual grain crops such as wheat, barley and rye. This implies that PhotoP_{base} would be lower
241 than PhotoP_{sat}. As for the STICS model, photoperiod effect was inactivated after flowering stage and
242 up to maturity.

243 2.3.4. Cold requirements

244 The cold requirement routine is a two-step procedure, in which the vernalizing value of a given day is
245 firstly computed (VV(i) in Eq.6), and then the slow-down factor SFV(i) is calculated as the ratio of
246 completion of the total vernalization requirements (Eq.7). We furthermore adapted the formalism
247 proposed in STICS to introduce a sensitivity parameter to vernalization, as for Eq. 5, to determine
248 what would be the degree of sensitivity of IWG to vernalization requirement.

249

250
$$VV(i) = \max\left(1 - \left[\frac{T_{vern} - T_{mean}(i)}{Ampli_{vern}}\right]^2, 0\right) \quad \text{Eq. 6}$$

251

252
$$\begin{cases} SFV(i) = \frac{[\sum_{j=D_{emer} \text{ or } D_{harv}}^i VV(j)] - VV_{min}}{VV_{req} - VV_{min}} \\ SFV(i) = \max(\min(SFV(i), 1), 0) \end{cases} \quad \text{Eq. 7}$$

253

254

255 In these equations, T_{vern} is the temperature to reach an optimal vernalization value during a given
 256 day, $Ampli_{vern}$ is the amplitude of the vernalizing effect, D_{emer} and D_{harv} are respectively the day of
 257 emergence (during the IWG establishment year) or the day of the last harvest (for any other year),
 258 VV_{min} is the minimum number of vernalizing days (fixed at 1 for this analysis) and VV_{req} is the total
 259 number of required vernalizing day . As for Eq.5, the second term of Eq.7 ensures that SFV (i) is
 260 mathematically bounded between 0 and 1.

261

262 Therefore, once initiated ($\sum VV(i) > VV_{min}$), the vernalization routine proposed in STICS considers that
 263 the “resting state” during winter time is not total and allows for a partial accumulation of
 264 development units. Furthermore, in this formalism, incomplete vernalization requirements ($\sum VV(i) <$
 265 VV_{req}) would slow the development of crops but would thus allow evolving in the phenology, leading
 266 eventually to flowering and maturity at a slower rate, without stopping it and preventing ears to be
 267 fertile.

268

269 [2.3.5. Snow cover correction](#)

270 Due to their climatic conditions (climate type Dfb), Canadian sites are prone to significant snowfalls
 271 and snow cover during winter. As suggested by Jégo et al., (2014) using crop models in northern
 272 areas of Canada, Scandinavia or Russia requires accurately simulating the impacts of snow cover and
 273 soil freezing on soil processes, survival and growth of (perennial) crops. Snow cover indeed changes

274 the energy budget of the soil surface by increasing the albedo, reducing the soil heat flux and the
275 surface roughness, and modifying the soil temperature and water content profiles (Jégo et al., 2014).
276 In their paper, previous authors compared three snow modules, more or less complex in their
277 representation of snow accumulation and melting. As we did not require the same level of
278 complexity, we considered a simpler approach based on a simple temperature threshold (Eq. 8).
279 Based on records obtained at Winnipeg, Canada, experimental sites regarding air temperature and
280 soil temperature (Fig. 1), a bilinear model was adjusted (Eq. 8).

281

$$282 \quad \begin{cases} T_{corr}(i) = T_{mean}(i) & \text{if } T_{mean}(i) > 0^{\circ}C \\ T_{corr}(i) = 0.165 \cdot T_{mean}(i) & \text{if } T_{mean}(i) < 0^{\circ}C \end{cases} \quad \text{Eq. 8}$$

283

284 Within climate type Dfb, this correction ($R^2=0.369$) was considered sufficient to mimic the impact of
285 snow insulation, which in turn allowed proper estimates of the effective temperature sensed by the
286 crop during the effective period of vernalization. Based on existing snow model (Jego et al., 2014)
287 and the recorded data (Fig. 1), “0°C” was considered a robust and coherent threshold. It was
288 furthermore to constrain the regressions through the origins [0,0]. The slope of the trend on records
289 reported in the upper right quadrant of Fig. S1 was quite logically forced to 1, while the slope of the
290 trend on records reported in the lower left quadrant was fit through automatic regression, resulting
291 in a coefficient of 0.165.

292

293 **2.4. Crop model inversion**

294 **2.4.1. The DREAM sampling algorithm**

295 Since the works of Metropolis (Metropolis et al., 1953) and later Hastings (1970), Bayesian
296 approaches have greatly improved to sample the most relevant parameter posterior distribution,
297 notably through the use of Markov Chain Monte Carlo (MCMC) simulations (Metropolis et al., 1953).
298 While a lot of research was devoted to improve Metropolis-Hastings approach up to the late 1990’s,

299 algorithms remained long inefficient when confronted with very heavy tails posterior distribution and
300 with posterior model output prediction surfaces that contained multiple local optima. Based on Ter
301 Braak's work (2006), research was conducted that successively lifted the different limitations and
302 enhanced considerably the efficiency of Bayesian MCMC genetic sampling procedures. The
303 Differential Evolution Adaptive Metropolis (DREAM) algorithm developed by Vrugt et al. (2009) is a
304 follow-up of the DE-MC method (Ter Braak, 2006), and integrates the advantages of the Shuffled
305 Complex Evolution Metropolis (SCEM-UA) global optimization algorithm (Vrugt et al., 2003).
306 The DREAM algorithm is probably one of the most advanced MCMC algorithms. Detailed descriptions
307 of the DREAM algorithm have been published, e.g. in Vrugt et al. (2009) and Vrugt (2016). Recently,
308 Dumont et al. (2014) coupled for the first time the DREAM algorithm with a complex crop model
309 (STICS in this case). This section presents a summary of the algorithm but we refer to papers for a
310 detailed description.

311

312 The advantages of DREAM are summarized here:

- 313 ▪ DREAM incorporates a self-adaptive randomized subspace sampling routine;
- 314 ▪ It can maintain a detailed balance and ergodicity that has proven effective to accommodate a
315 heavy-tailed and multimodal target;
- 316 ▪ It solves limitations such as the need to choose the starting values and the unlimited number
317 of parameters that could be optimized at the same time;
- 318 ▪ By integrating a formal approach to specify the likelihood function and explicitly consider the
319 residual errors statistical model, DREAM allows separation of behavioural solutions from
320 non-behavioural ones.

321 The last characteristic has been proven particularly effective in the case of crop model parameter
322 sampling (Dumont et al., 2014). Indeed, in agricultural research, the (model) errors are most of the
323 time correlated, non-stationary and non-Gaussian. As stated by Wallach et al. (2006), site-year
324 characteristics have a strong influence on observations and observations/model errors. When several

325 measurements are performed at different dates in a given site-year, observations and (model)
326 residuals will most often be auto-correlated.

327 2.4.2. Sampling procedure

328 With regard to the DREAM options, the toolbox ran a maximum of 5,000 evaluation functions
329 multiplied by the number of sampled parameters. Preliminary tests concluded that convergence was
330 easily ensured with such a rule. The number of Markov chains was fixed at two times the number of
331 parameters to be sampled, following Vrugt et al. (2009). Following the observation made by Dumont
332 et al. (2014), to improve the convergence of the algorithm when coupled with a crop model, a
333 standard error was considered on recorded data to compute the likelihood function. It was decided
334 to use a fixed sigma of 5 days, which is among the greatest standard error generally observed at
335 BBCH 65 due to the temporal sprawl of the flowering stage. Other options of the DREAM toolbox
336 were kept as the original release.

337

338 The initial values and the prior distribution were determined as specified in Table 1, based on
339 parameters as defined within the STICS model, literature review (Table S1) or expert knowledge.
340 Other parameters of the phenology model were kept at a fixed value: DT_{opt} and DT_{max} were
341 respectively fixed at 35 and 45°C, and VV_{min} was fixed at 1 equivalent-day

342

343 **Table 1** : Table of the parameter being optimised

Parameter	Initial value	A priori	Origin of the initial value
DT_{min}	0	[0 - 15]	Grassland / Wheat STICS parameter
VV_{req}	35	[20 - 100]	Grassland STICS parameter
T_{vern}	5	[-5 - 15]	Ryegrass STICS parameter
$Ampli_{vern}$	7.5	[1 - 20]	Ryegrass STICS parameter
$PhotoP_{base}$	8	[1 - 12]	Grassland / Wheat STICS parameter
$PhotoP_{sat}$	20	[13 - 24]	Grassland / Wheat STICS parameter
$\Sigma UPVT_{BBCH30}$	215	[0 - 600]	Preliminary test
$\Sigma UPVT_{BBCH39}$	345	[200 - 1000]	Preliminary test
$\Sigma UPVT_{BBCH65}$	700	[400 - 1200]	Preliminary test
$\Sigma UPVT_{BBCH89}$	1500	[800 - 2000]	Preliminary test

344

345

346 2.4.3. Data analysis and parameter uncertainty

347 Assessing the posterior distribution of the model parameters using MCMC simulations, as performed
348 with DREAM, lead to several chains that contained all the necessary information about model
349 parameters.

350 We first analyzed the marginal posterior distribution function (PDF) to retrieve the main information
351 regarding sampled parameters, i.e. the posterior means, medians, the main percentiles. We
352 furthermore looked at the correlation coefficients between the generated parameter samples. To do
353 so, the last 500 values of each chain, where stationarity had been achieved, were kept to process
354 data.

355 To further use the crop model as research or decision-support tools, it is necessary to summarize the
356 marginal posterior probability distribution function (PDF) in one parameter estimate. A first solution
357 would be to select, among the chains, the parameter set that offers the optimal solution, i.e. the one
358 that optimizes the convergence criterion. However, provided convergence has achieved a stationary
359 distribution, from a statistical/methodological point of view, the information contained in each chain

360 has statistically the same relevance. It was therefore decided to use the medians of the distributions
361 to evaluate the overall model performance.

362 2.4.4. Assessment of model performance

363 There is a need to define criteria that will help determine whether or not a model is ‘acceptable’, in
364 pursuit of set objectives and its ability to represent reality (Loague and Green, 1991). Three main
365 statistical criteria were used to assess model performance namely the root mean square error
366 (RMSE), the model efficiency (EF) and the normalized deviation (ND). These criteria are defined in
367 equations 9, 10 and 11.

$$368 \quad RMSE = \sqrt{\frac{1}{n} \sum_{i=1}^n (y_i - \hat{y}_i)^2} \quad \text{Eq. 9}$$

$$369 \quad EF = 1 - \frac{\sum_{i=1}^n (y_i - \hat{y}_i)^2}{\sum_{i=1}^n (y_i - \bar{y})^2} \quad \text{Eq. 10}$$

$$370 \quad ND = \frac{\sum_{i=1}^n (\hat{y}_i) - \sum_{i=1}^n (y_i)}{\sum_{i=1}^n (y_i)} \quad \text{Eq. 11}$$

371

372 In these equations, n is the number of observations, y_i is the i^{th} observation, \bar{y} is the average of
373 observation and \hat{y}_i is the simulated value corresponding to the i^{th} observation.

374 RMSE, EF and ND are rarely used alone for evaluating model quality. Different authors (Beaudoin et
375 al., 2008; Brisson et al., 2002; Dumont et al., 2014) used RMSE, EF and ND jointly, on the basis that
376 model calibration or validation is accurate if the RMSE is relatively low compared with the mean of
377 the observations, and if $EF > 0.5$ and $|ND| < 0.1$

378 2.4.5. Iterative process-based modelling approach

379 The crop model-based approach was used to pursue a two-fold objective

- 380 ▪ First, following the literature regarding IWG (Mitchell et al., 1998, Ivancic et al, under
381 review), the added-value of improving the temperature-driven phenological model with
382 vernalization and photoperiod processes was assessed. Each process was activated
383 sequentially. At each step, all model parameters related to the respectively activated
384 formalisms were optimized on all site-year combinations (Table S2), including the data sets

385 dedicated to validation. However, the data treatment was only focused on the global model
386 performance. The idea driving this phase was to determine whether or not IWG phenological
387 modelling demonstrated sensitivity to these processes, which would in turn corroborate the
388 findings of field and controlled experiments.

389 ▪ In a second phase, once the sensitivity of IWG phenological modelling to vernalization and
390 photoperiod was determined, an actual calibration/validation process was launched. All
391 relevant parameters were considered for sampling. In this second phase, data sets were
392 respectively dedicated to either calibration or validation, as per Table S2. The objective of
393 this phase was to create additional knowledge on IWG phenological development, by
394 retrieving the most probable value of the parameters controlling the developmental
395 processes.

396

397 **2.5. Software availability**

398 The software programs (this phenological model and DREAM) are libraries of Matlab® functions. The
399 full version of the current release of the STICS soil-crop model is accessible at
400 https://www6.paca.inrae.fr/stics_eng/. The functions of the phenological model presented in this
401 paper, which shares similarities with the STICS model, can be obtained by contacting the authors
402 (benjamin.dumont@uliege.be). The DREAM source codes were obtained from the developer
403 (jasper@uci.edu). Interested users should contact him directly.

404

405 3. Results

406 **3.1. Growing-degree day accumulation to flowering from February 1 base 0°C**

407 **Table 2.** Growing degree day accumulation from February 1 to flowering (base 0)

Regions and climate type	GDD accumulation range	Mean (different letters denote statistical differences across means)
Europe, Cfb climate	1527-1885	1628.9c
Canada, Dfb climate	952-1379	1160.2a
USA, Dfa climate	1234-1610	1436.5b

408

409 Computing GDD accumulation from Feb 01 to flowering (using the simpler formalization of eq. 1 and
410 2) demonstrates a large variability (from 952 to 1885) between fields and years. These values cover
411 most of the GDD range proposed by Cruz et al. (2010), hence belonging either to *early*, *medium*, or
412 *late forage grass species*. Meanwhile, values are however clustered by growth regions. European
413 conditions (Cfb Koppen climate classification) show the highest GDD values, while Canadian
414 conditions (Dfb) represent the lowest and USA (Dfa) provides intermediate values. Therefore, GDD
415 values are more likely relevant at a given regional scale to identify a plant growth pattern within the
416 region, rather than useful to characterize the overall plant phenological drivers. This latter
417 consideration highlights the need for more refined tools to simulate and evaluate IWG phenological
418 growth.

419

420 **3.2. IWG sensitivity to vernalization and photoperiod induction processes**

421

422 First, the crop model approach (including an intermediate step of parameter sampling) was used to
423 determine whether or not the temperature-driven phenological model would benefit from the
424 vernalization and photoperiod response processes to reproduce the observations. Table 3 reports
425 the overall model performances. The poor performance of the sole GDD_t formalization confirms

426 results presented at previous section. Adding the sole photoperiodic effect (SFP) did not improve
 427 sufficiently the model performance; RMSE was marginally decreased and model efficiency remained
 428 below the 0.5 threshold. The greatest improvement to model performance appeared when the
 429 vernalization process was activated (SFV). As observed, RMSE reached 10.06 days and model
 430 efficiency increased up to 0.97. Finally activating the photoperiod response function in addition to
 431 the SFV provided an additional improvement in model performance, with the RMSE dropping to 7.5
 432 days and model efficiency increasing slightly (0.98). At each step, a value of ND close to 0 is showing
 433 the algorithm tendency to avoid any under or overestimation (minimization of RMSE).

434

435 **Table 3.** Overall model performances considering the two induction processes

Model formalism	Model Performance		
	RMSE	EF	ND
GDD _t	57.49	-0.06	0.00
GDD _t × SFP	48.95	0.23	0.00
GDD _t × SFV	10.06	0.97	0.00
GDD _t × SFV × SFP	7.68	0.98	0.00

436

437

438

439 **3.3. Posterior distribution of crop parameters and model validation**

440 Table 4 summarizes the main descriptor of the posterior distribution function of the different
 441 parameters, namely the best parameter set, the median parameter set and its 10%-90% confidence
 442 interval. Table S3 presents the correlation matrix between the parameters.

443

444 **Table 4.** Descriptor of the posterior distribution function

Parameter	Best	Median	CI [10%-90%]
DT_{min}	0.35	0.49	[0.059 - 1.002]
VV_{req}	71.90	66.97	[36.116 - 79.378]
T_{vern}	4.64	4.49	[2.94 - 5.387]
$Ampli_{vern}$	7.43	7.09	[5.296 - 8.452]
$PhotoP_{base}$	9.65	9.99	[9.369 - 10.821]
$PhotoP_{sat}$	17.90	17.33	[15.687 - 22.336]
$\Sigma UPVT_{BBCH30}$	212.26	191.26	[127.534 - 260.885]
$\Sigma UPVT_{BBCH39}$	392.14	413.15	[282.854 - 537.153]
$\Sigma UPVT_{BBCH65}$	859.03	877.51	[601.251 - 1112.863]
$\Sigma UPVT_{BBCH89}$	1585.56	1622.31	[1354.823 - 1865.226]

445

446 Among the parameters optimized, DT_{min} tends towards “0” indicating that no growth is achieved
447 below this value, as found in other crops and grasses. T_{vern} indicates the optimal vernalization
448 temperature is reached around 4.6°C, which tends to be similar or lower than other temperate
449 forage grasses or annual grain crops. $Ampli_{vern}$ indicated that vernalizing conditions are (partially) met
450 between ~ -2.8 and $\sim +12^\circ\text{C}$. The total cold requirements (VV_{req}) were found to be equal to 58 days,
451 which would be a more grass-like type (Table S1), since most annual grain crops are capable of
452 vernalization with shorter cold periods. However, it is worth mentioning that some annual cultivars
453 of winter wheat might require a similar amount of vernalizing days (Gate, 1995). Finally, we found
454 that photoperiod was unlocked starting at 9.7 hours and would not be limiting anymore over 17.9
455 hours of daylength. This daylength range implies that the SFP formalism takes a value of 0.5 around
456 11.8h daylength, and 1 at 13.8h daylength. Overall, the optimized parameters confirm the relevance
457 of a temperature-daylength coupled formalism to represent IWG phenological development under
458 various growing conditions.

459 The correlation matrix (Table S3) indicates the level of correlation between parameters during the
460 optimization process. A strong interdependency is observed between the sums of UPVT, which are
461 also strongly correlated to $PhotoP_{sat}$. The limited contrast on upper photoperiod values in the dataset

462 generates uncertainty on the parameter $\text{PhotoP}_{\text{sat}}$, that leads to lower reliability on the different
463 ΣPVT due to the high correlation of both parameters. This might be solved by integrating new
464 observations gathered at Northern sites (e.g. Sweden), to precisely determine the saturation upper
465 limit of the photoperiod effect.

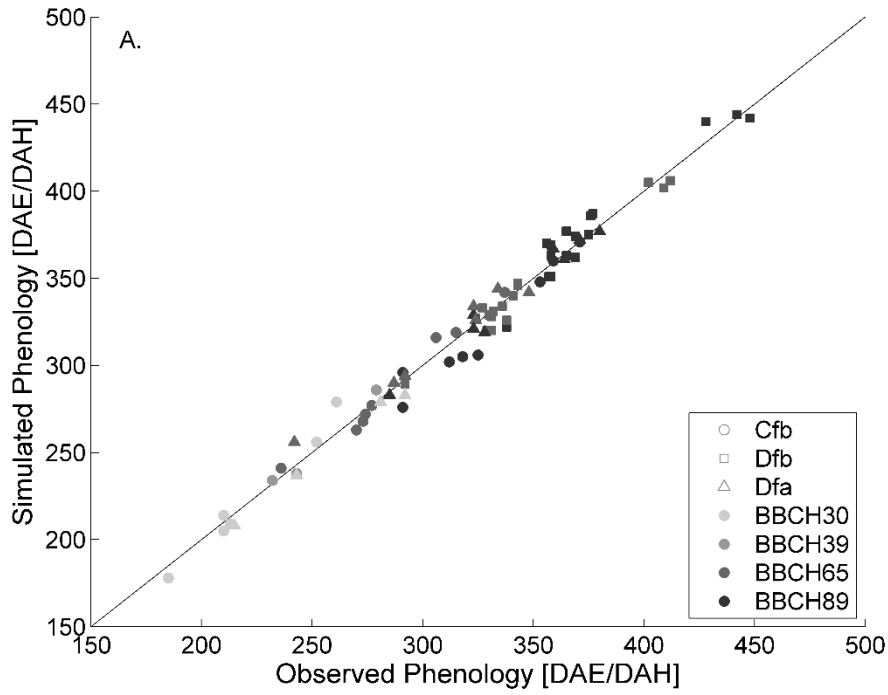
466 The model exhibited high performance both under calibration and validation datasets (Fig. 1 and
467 Table 5). The RMSE were respectively of 7.7 and 7.8 days, which respectively corresponded to a 2.4%
468 and 2.5% RRMSE (RMSE relative to the average of respective observations) in both cases. Model
469 efficiencies were close to 1, which is the upper theoretical threshold, indicative of a near perfect fit
470 of the model against observations. Finally, the normalized deviations, which indicate the tendency to
471 over- or underestimate observations, were very close to "0" and far below the 0.1 acceptance
472 threshold. As can be seen in Fig. 3, the simulated phenology (DAE/DAH at which the stage is
473 supposed to occur) is almost perfectly aligned on the 1:1 line with the observed phenology.

474 **Table 5:** Model performances under the calibration and validation steps

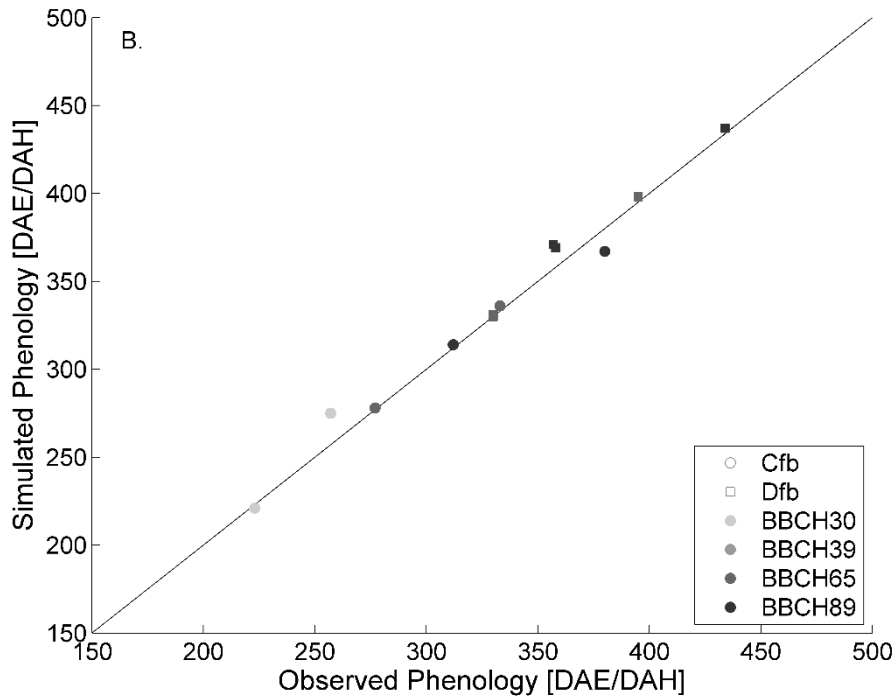
Criteria	<i>Calibration</i>	<i>Validation</i>
RMSE	7.562	8.401
EF	0.982	0.978
ND	-0.001	0.010

475

476



477

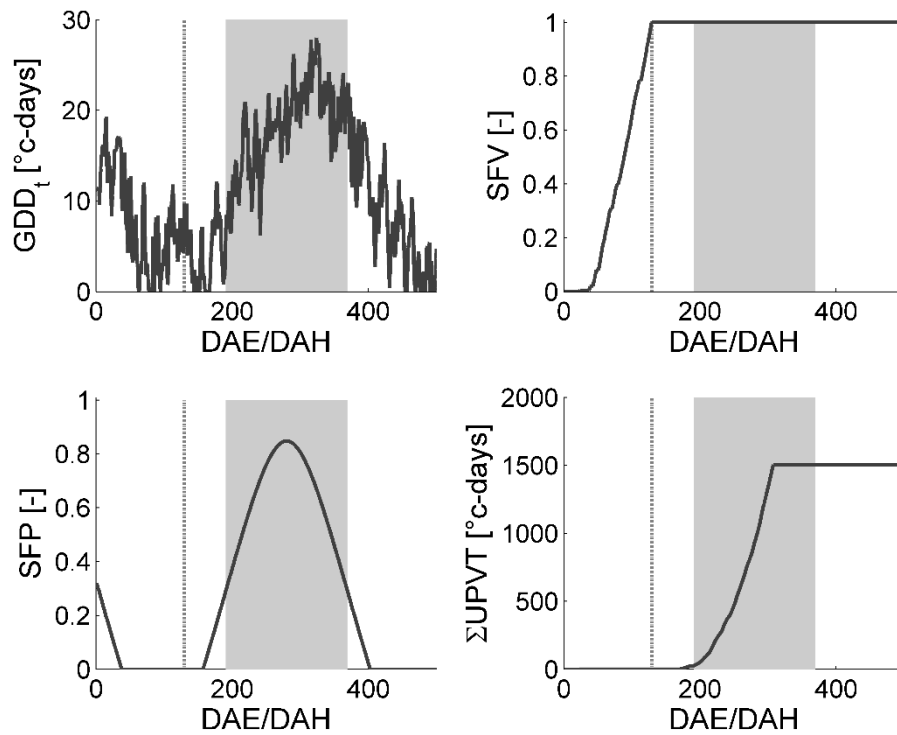


478

479 **Figure 1:** Observed and simulated phenology for the calibration (A) and validation (B) datasets. Climate type Cfb is
 480 represented by circles (o), climate type Dfb is represented by squares (□) and climate type Dfa is represented by triangle
 481 (Δ). Intensity of grey varies with simulated crop stage in BBCH scale, with lighter grey being stem extension (BBCH 30) and
 482 darker grey being maturity (BBCH 89).

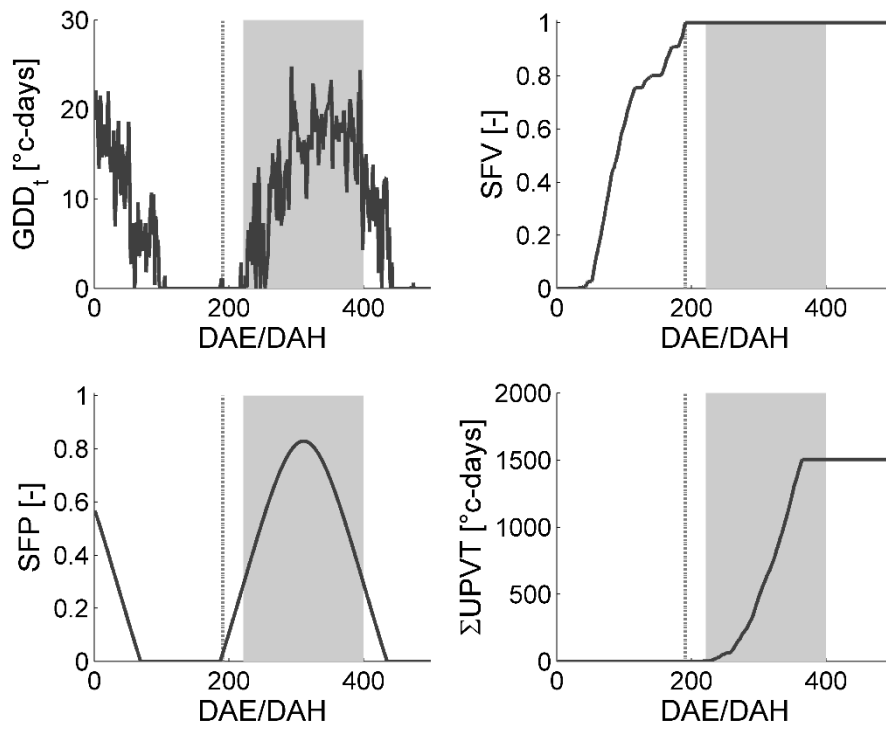
483

3.4. Development dynamics from different sites and limiting environmental conditions



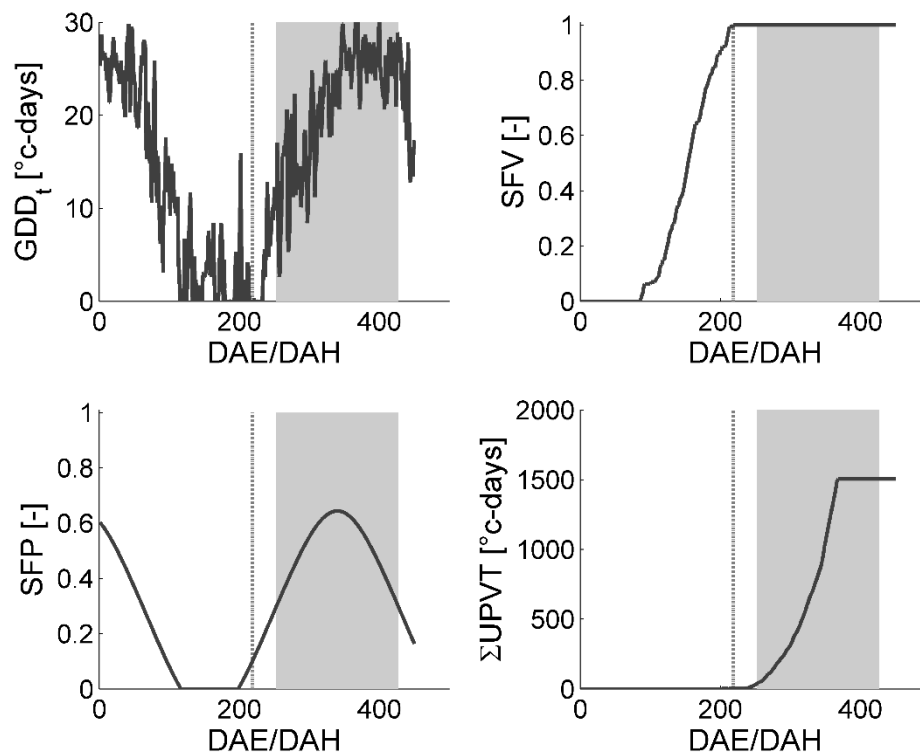
485

486 **Figure 2:** Simulated GDD_t (Growing-Degree-Day), SFV (Slowdown Factor accounting for Vernalization), SFP (Slowdown
 487 Factor accounting for Photoperiod) and UPVT (Photo-Vernalo-Thermic Units) for the Maubec French site (validation site)
 488 over the season 2018 (establishment year). Light grey dashed line represents the day where cold requirement is fully met.
 489 Light grey shaded area represents the period for which SFP is greater than 0.3 (>11h daylength). UPVT accumulation was
 490 stopped when maturity was reached.



491

492 **Figure 3:** Simulated GDD_t (Growing-Degree-Day), SFV (Slowdown Factor accounting for Vernalization), SFP (Slowdown
 493 Factor accounting for Photoperiod) and UPVT (Photo-Vernal-Thermic Units) for the Carman-LN Canadian site (validation
 494 site) over the season 2017 (second growing year). Light grey dashed line represent the day where cold requirement is fully
 495 met. Light grey shaded area represent period for which SFP is greater than 0.3 (>11h daylength). UPVT accumulation was
 496 stopped when maturity was reached.



497

498 **Figure 4:** Simulated GDD_t (Growing-Degree-Day), SFV (Slowdown Factor accounting for Vernalization), SFP (Slowdown
 499 Factor accounting for Photoperiod) and UPVT (Photo-Vernalo-Thermic Units) for the Salina US site (calibration site) over
 500 the season 2017 (second growing year). Light grey dashed line represents the day where cold requirements is fully met.
 501 Light grey shaded area represents the period for which SFP is greater than 0.3 (>11h daylength). UPVT accumulation was
 502 stopped when maturity was reached.

503

504 Comparing the two validation sites (Maubec-18: Cfb climate, and Carman-LN-17: Dfb climate) and
 505 one calibration site (Salina: Dfa climate), the dynamic of UPVT accumulation is expressing the
 506 combined status of the SFV, SFP and GDD parameters. The period of UPVT accumulation between
 507 sites indicates the development of reproductive growth of *Th. intermedium*, which correspond to the
 508 progression from BBCH30 to BBCH89 stages.

- 509 • Under Cfb climate (temperate European conditions, e.g. Maubec-18, Fig. 2), fulfillment of
 510 vernalization requirements was reached in early January (~140 DAE) after around 90 days of
 511 SFV accumulation. However, UPVT accumulation encompasses a period of about 110 days
 512 corresponding to the period between March and July. Despite early GDD accumulation, the

513 SFP coefficient was below 0.3 (<11h daylength) until 200 DAE (mid-March), strongly limiting
514 UPVT accumulation. This would represent a period of about two months between
515 vernalization achievement and significant reproductive growth, which means early
516 development and secondary induction of *Th. intermedium* was limited by the photoperiod
517 mediation and short daylength.

518 • Under Dfb climate (Canadian conditions, e.g. Carman-LN-17, Fig. 3), fulfillment of
519 vernalization requirements was reached in March (~190 DAH) after around 140 days of SFV
520 accumulation. UPVT accumulation encompasses a period of about 150 days corresponding to
521 the period between April and September. This start of reproductive growth corresponds to
522 both the start of GDD accumulation and the increased daylength (>11h, grey zones in the
523 figure 6.) In other words, *Th. intermedium* early development (prior to April) would have
524 been limited by both GDD and short daylength, indicating a notable temperature-daylength
525 coupling.

526 • Under Dfa climate (continental US conditions, e.g. Salina-19, Fig. 4): fulfillment of
527 vernalization requirements was also reached in March (~210 DAH) after around 120 days of
528 SFV accumulation. UPVT accumulation encompasses a period of about 130 days
529 corresponding to the period between April and July. The start of reproductive growth
530 corresponds to the increased daylength (>11h, grey zones in Fig 7.), while GDD was never the
531 limiting factor. In other words, *Th. intermedium* early development would have been mostly
532 limited by short daylengths.

533 4. Discussion

534 4.1. Tiller primordia induction (primary induction)

535 *Th. intermedium* appears to be highly dependent on the vernalizing process. The requirements for
536 low temperatures (LT) is almost mandatory for tiller induction, but our study was not calibrated to
537 uncover the potential influence of contrasted daylength (SD-LD) on these requirements. With

538 vernalizing temperatures between -2.8 and 12 °C (optimum at 4.6°C ; in keeping with Ivancic et al.,
539 *under review* ; Table 4), LT requirements are similar to winter cereal grain crops and other
540 vernalizing cool-season grasses (*Lolium perenne*, *Festuca pratensis*, *Poa pratensis*, *Agrostis capillaris*)
541 (Table S1), although certain species would have greater vernalizing success than IWG under cooler
542 temperatures (e.g. *Dactylis glomerata*, *Bromus inermis*), shorter periods of exposure (annual grains),
543 or longer periods of exposure (other perennial grasses). Depending on climatic conditions, earliness
544 of vernalization fulfillment might differ significantly and substantially influence dormancy break.
545 Considering the large and general trend where LD increase LT requirements (if not inhibiting) in
546 various vernalizing grasses, we can hypothesize that *Th. intermedium* would behave similarly (Heide,
547 1987, 1984) and might require an increased vernalization treatment under longer daylengths.

548

549 Interestingly, no significant discrepancy was observed at the sward level in the phenology model
550 between the different germplasm origins (TLI, UMN) and breeding cycles tested (TLI-C3, C4, C5).
551 Among the populations considered, it is notable that the Canadian sites grew experimental
552 populations that were *de facto* selected for increased winter survival capacity (Cattani, 2017; Cattani
553 and Asselin, 2018b). Therefore, their similar fitness with respect to the phenology model indicates
554 that either: i) cold tolerance of *Th. intermedium* may not be tightly linked to the vernalization
555 process (Seppänen et al., 2013); and/or ii) differences in vernalizing requirements were too subtle to
556 be detected; and/or iii) the integration of winter snow-cover into the model, and the induced air
557 temperature corrections, masks a potential discrepancy.

558

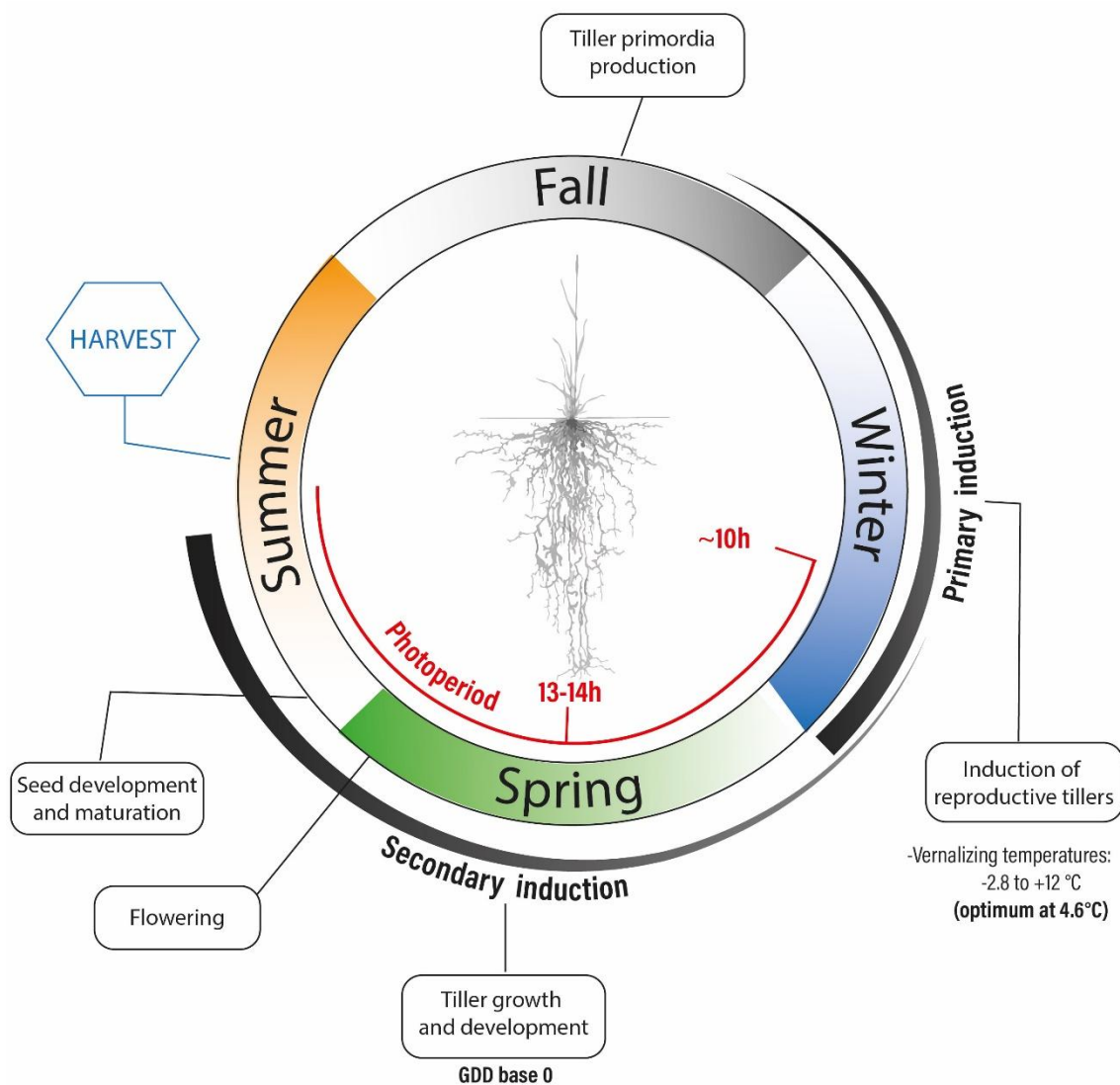
559 4.2. Tiller growth and flowering (secondary induction)

560 Following vernalization achievement, the accumulation of heat units (GDD base 0 ; Table 4) that
561 triggers break of dormancy, plant growth and flowering were strongly associated with a photoperiod-
562 mediated process (Fig. 5). Such daylength induction confirms that primary induction must be
563 followed by a secondary induction - including daylength responsiveness - that starts the reproductive

564 growth period (stem elongation and flowering). Across all sites and years, initiation of anthesis was
565 observed between June 14 and July 2. In spite of the contrasted growing conditions and accumulated
566 GDD reported in Table 2, this relatively synchronized flowering period, would confirm the influence
567 of photoperiod regulation on growth rate and demonstrate the misrepresentation of GDD concept
568 alone to explain *Th. intermedium* phenological development in the various growing regions.

569 Such a photoperiod mediation process is widely known and observed in forage grasses and cereal
570 grains, but the degree of sensitivity varies. The proposed phenological model indicates the potential
571 for reproductive growth between 9.7 and 17.9h daylength (Table 4), but we noted that new
572 observations on Northern regions would likely lower the saturation upper limit of the photoperiod
573 effect. According to the demonstration of UPVT accumulation (Fig 2, 3, 4), plant phenological
574 development from BBCH30 generally began around 11h of daylength. Earlier development was
575 however possible with temperatures above 0°C, but was strongly limited due to the combination of
576 low GDD and SFPI coefficient <0.3, or may have resulted in vegetative growth rather than
577 reproductive tiller development. Between 13 and 14h daylengths, plant development was not
578 limited by the photoperiodic response and was fully associated with GDD accumulation.

579



580

581 **Figure 5:** *Thinopyrum intermedium* phenological development milestones and environmental drivers. (with colors)

582

583 4.3. Tiller elongation: a crucial context-dependent trait to manage production

584 In production fields, flowering earliness is a critical factor since it provides a good representation of
 585 the whole growth cycle timing and stages (Ansquer et al., 2009a), driving the field operations agenda
 586 (e.g. fertilization). In spite of the variability of flowering earliness due to different growth rates and
 587 stem elongation, particularly influenced by N availability, the calculation of GDD under similar
 588 climatic and daylength contexts has been demonstrated as a robust method to predict flowering
 589 periods of different cool-season forage grasses (Ansquer et al., 2009a). Therefore, it has been

590 accepted as one of the main criteria that distinguish different plant growth strategies under similar
591 situations and low-input systems (Ansquer et al., 2009a; Cruz et al., 2010; Duru et al., 2009).

592

593 Under French and Belgium temperate conditions, GDD calculation until flowering (Table 2) indicate
594 that *Th. intermedium* belongs to the slow-growing and more 'conservative' plants commonly found in
595 these regions (e.g. *Brachypodium sp.*, *Agropyron sp.*, *Deschampsia cespitosa*, *Phleum pratense*)
596 compared to earlier plants (e.g. *Alopecurus pratense*, *Lolium perenne*, *Festuca pratense*). These later
597 flowering species are generally characterized by taller stands, longer leaf lifespan, lower leaf area per
598 mass unit, lower leaf nitrogen concentration and relative growth rate (Ansquer et al., 2009b; Cruz et
599 al., 2010; Duru et al., 2005, 1995; Ryser and Lambers, 1995). In low input fields, slow establishment
600 and a slow growing canopy can result in weed infestations and poor grain filling in dry conditions in
601 late summer. As a result, slow-growing species like IWG may be better suited to higher altitude fields
602 or higher latitude situations often characterized by delayed growth season.

603

604 On the other hand, the *Th. intermedium* flowering period in the North American continental context
605 might be seen as relatively early (lower GDD accumulation) compared to warm-season grasses
606 *Panicum virgatum*, *Andropogon gerardii* and *Sorghastrum nutans* commonly found under harsh
607 growing conditions of the *Northern Great Plains Tallgrass Prairie*. Those species are described as very
608 conservative, capable of high biomass production and very efficient in nitrogen recycling and use
609 (Friesen and Cattani, 2017). Conversely, *Th. intermedium* would require higher nitrogen
610 concentration and require more nitrogen availability to ensure optimal reproductive growth under
611 similar conditions. Compared to warm-season grasses, the more acquisitive traits of *Th. intermedium*
612 would be favorable to quicker plant growth and establishment in fields in situations of suitable
613 resource availability.

614

615 If vernalization is more quickly achieved under Cfb climate, the timing of secondary induction relative
616 to the loss of cold hardiness in the spring could be the difference in observed response between
617 Western Europe and the Northern Great Plains of North America and its continental climate. If a
618 plant loses its cold acclimation and the plant has yet to reach the inductive day length (or gdd
619 accumulation combination), nutrients and water may be used for new vegetative tiller recruitment.
620 Internode elongation will be both energy and water demanding. When induction conditions are met,
621 nutrients (including water) may be diverted from reproductive growth to support excessive
622 vegetative growth, reducing seed yield. Thus, timing of secondary induction and spring regrowth will
623 be critical to optimizing the response to fertilization. For instance, if dormancy is broken and growth
624 begins potentially in February (in France) and the flowering response is primarily to longer days
625 (>13hr daylength), the pre-reproductive growth will be much longer duration than in Manitoba,
626 Canada, where cold tolerance and dormancy will still be intact at that time of year. Therefore, growth
627 will appear to be quicker in Manitoba as less time, if any, elapses between the resumption of growth
628 in the spring and the onset of reproductive growth.

629 Under situations with prolonged non-reproductive growth after winter time, as observed in western
630 European conditions, the ability of other species to respond to early fertility boost and grow
631 reproductively may provide an advantage to weed species, e.g. perennial ryegrass (*Lolium perenne*).
632 Selection for earlier flowering in these growth environments, potentially achieved through different
633 and possibly interrelated methods (e.g. reducing phyllochron through reduced leaf length and
634 appearance rate, or by altering daylength requirements) would then alter this timing relationship,
635 and should move anthesis earlier in the growing season and potentially reduce the stressful
636 influences from a later secondary induction timing. Extreme heat during anthesis, as experienced in
637 France in 2019, is an excellent example of the risks of later flowering that can exacerbate already
638 reduced grain yields of this new perennial crop.

639

640 The flowering induction process is critical to understanding environmental requirements that support
641 *Th. intermedium* reproductive growth, however it is primarily relevant when linked to flowering and
642 reproductive growth rate traits within a specific growth situation. The understanding of the
643 phenology will therefore inform agronomic practices.

644

645 4.4. Scaling up the use of *Th. intermedium* grain production by designing and pairing 646 ecotypes with geographies for optimized flowering induction

647 Model compliance is based on IWG overall sward growth, without taking inter- and intra-individual
648 heterogeneity into account. However, individual discrepancy in flowering period has been observed
649 within fields. The observation of slower tillers, with delayed heading and flowering, calls for further
650 research on axillary bud production and induction, linked to vegetative growth periods and resource
651 availability dynamics. Also, with spring seedings, flowering in summer has been observed without
652 previous winter vernalization, although seed harvest would not be profitable due to the timing and
653 the limited amount of flowering observed. Such heterogeneity is regularly observed in perennial
654 grasses, and might indicate a potential breeding opportunity to develop ideotypes with favorable
655 phenology for specific target populations of environments. In the meantime, the effect of reducing
656 population diversity must be taken into account in order to define appropriate thresholds that
657 maintain the benefits of population diversity in fields (e.g. resilience, longevity). Breeding for a more
658 uniform ideotype may alter plant growth and might expose the crop to other issues not historically
659 associated with the species. For example, greater *Th. intermedium* earliness in breaking in dormancy
660 in the spring carries the risk of injury under later occurring adverse climatic conditions or seed
661 productivity decline (Cattani, 2017). Likewise, breeding toward more acquisitive plant traits
662 associated with quicker growth may also bring new drawbacks such as increased disease problems
663 (increased leaf moisture), reduced longevity or increased susceptibility to drought. More
664 conservative plants typically have higher water use efficiency (De Oliveira et al., 2019, 2018), while
665 acquisitive plants utilize water quickly to grow rapidly.

666 Influence of management practices such as fertilization illustrates the plasticity of acquisitive-
667 conservative plant functional types in managed growth environments, which potentially can be very
668 different in terms of resource availability, competitive interactions and climatic effects as compared
669 to the native growth habitat of the plant. Among the most studied practices, nitrogen fertilization of
670 forage grasses, was shown to be responsible for improving leaf elongation rate and leaf area (Gastal
671 and Durand, 2000) thus potentially impacting the overall plant growth rate, assimilation, and tillering
672 (Mitchell et al., 1998; Poorter and Remkes, 1990; Shipley, 2006; Simon and Lemaire, 1987). Similarly,
673 the management of defoliation practices might widely influence plant growth, notably due to
674 influence on carbon and nitrogen fluxes and reserves (Ferraro and Oesterheld, 2002; Gastal et al.,
675 2010; Gastal and Lemaire, 2015; Hunter et al., 2020; Medina-Roldán and Bardgett, 2011). The usually
676 large ontogenic plasticity of forage grasses also reinforces the influence of defoliation, which result in
677 disturbed phytomers. According to Nelson (2000), most cool-season grasses demonstrate
678 interrelated vegetative (leaf) growth and tillering, whereas vegetative growth improvement
679 (biomass) generally reduces tillering and lengthens the phyllochron, likely due to increased light
680 interception and competition to the detriment of axillary (tiller) bud activation (Simon and Lemaire,
681 1987). Thus, significant non-reproductive growth under favorable environmental conditions might
682 ultimately lead to fewer tillers. This would be similar to observed situations under aging (three-four
683 years old), or “sod-bound” *Th. intermedium* stands, where tillering activity is strongly reduced
684 (Hunter et al., 2020; Tautges et al., 2018), and may require strategic canopy disturbance to maintain
685 reproductive tillers. Thus, a large field of research remains open to determine the interactions
686 between agronomic management and directed breeding, with plant plasticity, including reproductive
687 growth rate, timing and intensity, to optimize its reproductive potential.

688 5. Conclusion

689 This study shows that introducing a new grain crops from new genotype and ecotype pools requires a
690 broader assessment than only attention towards its yield potential. Here we show that vernalization,
691 followed by GDD-daylength coupled dynamics in spring, drives IWG sward functional changes,

692 potentially resulting in variable agronomic performances depending on growth environment and
693 cropping system management. Our results highlight the need to develop an integrative research
694 approach combining crop genetics, ecology and agronomy to improve our understanding of our
695 cropping systems as a whole.

696

697 6. Acknowledgement

698 We acknowledge all field technicians and scientists that contributed to create and assemble this
699 dataset. We also thank the reviewers for their usefull comments.

700

701 7. References

- 702 Aamlid, T., 2000. Primary and Secondary Induction Requirements for Flowering of Contrasting
703 European Varieties of *Lolium perenne*. *Annals of Botany* 86, 1087–1095.
704 <https://doi.org/10.1006/anbo.2000.1275>
- 705 Ansquer, P., Duru, M., Theau, J.P., Cruz, P., 2009. Functional traits as indicators of fodder provision
706 over a short time scale in species-rich grasslands. *Ann Bot* 103, 117–126.
707 <https://doi.org/10.1093/aob/mcn215>
- 708 Ansquer, P., Khaled, R.A.H., Cruz, P., Theau, J.-P., Therond, O., Duru, M., 2009. Characterizing and
709 predicting plant phenology in species-rich grasslands. *Grass and Forage Science* 64, 57–70.
710 <https://doi.org/10.1111/j.1365-2494.2008.00670.x>
- 711 Ansquer, P., Theau, J.-P., Cruz, P., Viegas, J., Al Haj Khaled, R., Duru, M., 2004. Caraceterisation de la
712 diversité fonctionnelle des prairies à flore complexe. Vers la construction d’outils de gestion.
713 *Fourrages* 179, 353–368
- 714 Bajgain, P., Zhang, X., Jungers, J.M., DeHaan, L.R., Heim, B., Sheaffer, C.C., Wyse, D.L., Anderson, J.A.,
715 2020. ‘MN-Clearwater’, the first food-grade intermediate wheatgrass (*Kernza* perennial grain)
716 cultivar. *J. Plant Regist.* 14, 288–297. <https://doi.org/10.1002/plr2.20042>
- 717 Bartholomew, P.W., Williams, R.D., 2005. Cool-Season Grass Development Response to Accumulated
718 Temperature under a Range of Temperature Regimes. *Crop Sci.* 45, 529–534.
719 <https://doi.org/10.2135/cropsci2005.0529>
- 720 Basu, S., Parya, M., Dutta, S.K., Jena, S., Maji, S., Nath, R., Mazumdar, D., Chakraborty, P.K., 2012.
721 Effect of growing degree day on different growth processes of wheat (*Triticum aestivum* L.).
722 *Journal of Crop and Weed*, 8, 18–22.
- 723 Beaudoin, N., Launay, M., Sauboua, E., Ponsardin, G., Mary, B., 2008. Evaluation of the soil crop
724 model STICS over 8 years against the “on farm” database of Bruyères catchment. *European*
725 *Journal of Agronomy* 29, 46–57. <https://doi.org/10.1016/j.eja.2008.03.001>
- 726 Brisson, N., Delecolle, R., 1992. Developpement et modeles de simulation de cultures. *Agronomie* 12,
727 253–263.
- 728 Brisson, N., Launay, M., Mary, B. (Eds.), 2009. Conceptual basis, formalisations and parameterization
729 of the STICS crop model, Quae. ed, Update Sciences and technologies.
- 730 Brisson, N., Mary, B., Ripoche, D., Jeuffroy, M.H., Ruget, F., Nicoullaud, B., Gate, P., Devienne-Barret,
731 F., Antonioletti, R., Durr, C., Richard, G., Beaudoin, N., Recous, S., Tayot, X., Plenet, D., Cellier, P.,
732 Mchet, J.-M., Meynard, J.M., Delécolle, R., 1998. STICS: a generic model for the simulation of
733 crops and their water and nitrogen balances. I. Theory and parameterization applied to wheat
734 and corn. *Agronomie* 18, 311–346. <https://doi.org/10.1051/agro:19980501>

735 Brisson, N., Ruget, F., Gate, P., Lorgeou, J., Nicoullaud, B., Tayot, X., Plenet, D., Jeuffroy, M.-H.,
736 Bouthier, A., Ripoche, D., Mary, B., Justes, E., 2002. STICS: a generic model for simulating crops
737 and their water and nitrogen balances. II. Model validation for wheat and maize. *Agronomie* 22,
738 69–92. <https://doi.org/10.1051/agro:2001005>

739 Brown, W.F., Moser, L.E., Klopfenstein, T.J., 1986. Development and validation of a dynamic model of
740 growth and quality for cool season grasses. *Agricultural Systems* 20, 37–52.
741 [https://doi.org/10.1016/0308-521X\(86\)90034-X](https://doi.org/10.1016/0308-521X(86)90034-X)

742 Casler, M.D., 2012. Switchgrass Breeding, Genetics, and Genomics, in: Monti, A. (Ed.), *Switchgrass,*
743 *Green Energy and Technology.* Springer London, London, pp. 29–53.
744 https://doi.org/10.1007/978-1-4471-2903-5_2

745 Castro, J.C., Boe, A., Lee, D.K., 2011. A Simple System for Promoting Flowering of Upland Switchgrass
746 in the Greenhouse. *Crop Science* 51, 2607–2614. <https://doi.org/10.2135/cropsci2011.03.0142>

747 Cattani, D., 2017. Selection of a perennial grain for seed productivity across years: Intermediate
748 wheatgrass as a test species. *Canadian Journal of Plant Science* 97.
749 <https://doi.org/10.1139/CJPS-2016-0280>

750 Cattani, Douglas, Asselin, S.R., 2018a. Has Selection for Grain Yield Altered Intermediate Wheatgrass?
751 *Sustainability* 10, 688. <https://doi.org/10.3390/su10030688>

752 Cattani, Doug, Asselin, S.R., 2018b. Extending the Growing Season: Forage Seed Production and
753 Perennial Grains. *Can. J. Plant Sci.* 98, 235–246. <https://doi.org/10.1139/CJPS-2017-0212>

754 Chauvel, B., Munier-Jolain, N., Letouzé, A., Grandgirard, D., 2000. Developmental patterns of leaves
755 and tillers in a black-grass population (*Alopecurus myosuroides* Huds.). *Agronomie* 20, 247–257.
756 <https://doi.org/10.1051/agro:2000124>

757 Chauvel, B., Munier-Jolain, N.M., Grandgirard, D., Gueritain, G., 2002. Effect of vernalization on the
758 development and growth of *Alopecurus myosuroides*. *Weed Research* 42, 166–175.
759 <https://doi.org/10.1046/j.1365-3180.2002.00276.x>

760 Chouard, P., 1960. Vernalization and its Relations to Dormancy. *Annual Review of Plant Physiology*
761 11, 191–238. <https://doi.org/10.1146/annurev.pp.11.060160.001203>

762 Cooper, J.P., Calder, D.M., 1964. The Inductive Requirements for Flowering of Some Temperate
763 Grasses. *Grass and Forage Science* 19, 6–14. <https://doi.org/10.1111/j.1365-2494.1964.tb01133.x>

765 Crews, T.E., 2016. Closing the Gap between Grasslands and Grain Agriculture. *Kan. JL & Pub. Pol’y* 26,
766 274.

767 Cruz, P., Theau, J.P., Lecloux, E., Jouany, C., Duru, M., 2010. Typologie fonctionnelle de graminées
768 fourragères pérennes: une classification multitraits. *Fourrages* 201, 11–17.

769 Davidson, J.L., Milthorpe, F.L., 1965. The Effect of Temperature on the Growth of Cocksfoot (*Dactylis*
770 *glomerata* L.). *Ann Bot* 29, 407–417. <https://doi.org/10.1093/oxfordjournals.aob.a083962>

771 De Oliveira, G., Brunzell, N.A., Crews, T.E., DeHaan, L.R., Vico, G., 2019. Carbon and water relations in
772 perennial Kernza (*Thinopyrum intermedium*): An overview. *Plant Science* 110279-
773 <https://doi.org/10.1016/j.plantsci.2019.110279>

774 De Oliveira, G., Brunzell, N.A., Sutherlin, C.E., Crews, T.E., DeHaan, L.R., 2018. Energy, water and
775 carbon exchange over a perennial Kernza wheatgrass crop. *Agricultural and Forest Meteorology*
776 249, 120–137. <https://doi.org/10.1016/j.agrformet.2017.11.022>

777 DeHaan, L., 2015. Perennial crops are a key to sustainably productive agriculture, in: *Food Security :*
778 *Production and Sustainability.*

779 DeHaan, L., Christians, M., Crain, J., Poland, J., 2018. Development and Evolution of an Intermediate
780 Wheatgrass Domestication Program. *Sustainability* 10, 1499.
781 <https://doi.org/10.3390/su10051499>

782 Dubcovsky, J., Loukoianov, A., Fu, D., Valarik, M., Sanchez, A., Yan, L., 2006. Effect of Photoperiod on
783 the Regulation of Wheat Vernalization Genes VRN1 and VRN2. *Plant Mol Biol* 60, 469–480.
784 <https://doi.org/10.1007/s11103-005-4814-2>

785 Duchene, O., Celette, F., Ryan, M.R., DeHaan, L.R., Crews, T.E., David, C., 2019. Integrating
786 multipurpose perennial grains crops in Western European farming systems. *Agriculture,*
787 *Ecosystems & Environment* 284, 106591. <https://doi.org/10.1016/j.agee.2019.106591>

788 Dumont, B., Leemans, V., Mansouri, M., Bodson, B., Destain, J.-P., Destain, M.-F., 2014. Parameter
789 identification of the STICS crop model, using an accelerated formal MCMC approach.
790 *Environmental Modelling & Software* 52, 121–135.
791 <https://doi.org/10.1016/j.envsoft.2013.10.022>

792 Durand, R., 1967. Action de la température et du rayonnement sur la croissance. *Ann. Physiol. Vég.*
793 5–27.

794 Duru, M., Al Haj Khaled, R., Ducourtieux, C., Theau, J.P., de Quadros, F.L.F., Cruz, P., 2008a. Do plant
795 functional types based on leaf dry matter content allow characterizing native grass species and
796 grasslands for herbage growth pattern? *Plant Ecology* 201, 421–433.
797 <https://doi.org/10.1007/s11258-008-9516-9>

798 Duru, M., Ducrocq, H., Tirilly, V., 1995. Modeling growth of cocksfoot (*Dactylis glomerata* L.) and tall
799 fescue (*Festuca arundinacea* schreb.) at the end of spring in relation to herbage nitrogen status.
800 *Journal of Plant Nutrition* 18, 2033–2047. <https://doi.org/10.1080/01904169509365042>

801 Duru, M., Justes, E., Langlet, A., Tirilly, V., Rouziès, S., Sos, L., Viard, R., 1993. Comparaison des
802 dynamiques d'apparition et de mortalité des organes de fétuque élevée, dactyle et luzerne
803 (feuilles, talles et tiges). *Agronomie* 13, 237–252. <https://doi.org/10.1051/agro:19930401>

804 Duru, M., Adam, M., Cruz, P., Martin, G., Ansquer, P., Ducourtieux, C., Jouany, C., Theau, J.P., Viegas,
805 J., 2008c. Modelling above-ground herbage mass for a wide range of grassland community
806 types. *Ecol. Model.* 220, 209–225. <https://doi.org/10.1016/j.ecolmodel.2008.09.015>

807 Duru, M., P, P.C., Raouda, A.H.K., Ducourtieux, C., Theau, J.P., 2008b. Relevance of Plant Functional
808 Types based on Leaf Dry Matter Content for Assessing Digestibility of Native Grass Species and
809 Species-Rich Grassland Communities in Spring. *Agronomy Journal* 100, 1622–1630.
810 <https://doi.org/10.2134/agronj2008.0003>

811 Duru, M., Tallowin, J., Cruz, P., 2005. Functional diversity in low input grassland farming systems:
812 characterisation, effect and management, in: *Integrating Efficient Grassland Farming and*
813 *Biodiversity*. Tartu, pp. 199–210.

814 Esbroeck, G.A.V., Hussey, M.A., Sanderson, M.A., 2003. Variation between Alamo and Cave-in-Rock
815 Switchgrass in Response to Photoperiod Extension. *Crop Science* 43, 639–643.
816 <https://doi.org/10.2135/cropsci2003.6390>

817 Esbroeck, G.A.V., Hussey, M.A., Sanderson, M.A., 1997. Leaf Appearance Rate and Final Leaf Number
818 of Switchgrass Cultivars. *Crop Science* 37, 864–870.
819 <https://doi.org/10.2135/cropsci1997.0011183X003700030028x>

820 Ferraro, D.O., Oesterheld, M., 2002. Effect of defoliation on grass growth. A quantitative review.
821 *Oikos* 98, 125–133. <https://doi.org/10.1034/j.1600-0706.2002.980113.x>

822 Fowler, D.B., Limin, A.E., Wang, S.-Y., Ward, R.W., 1996. Relationship between low-temperature
823 tolerance and vernalization response in wheat and rye. *Canadian Journal of Plant Science* 76,
824 37–42. <https://doi.org/10.4141/cjps96-007>

825 Frank, A.B., Bauer, A., 1995. Phyllochron Differences in Wheat, Barley, and Forage Grasses. *Crop*
826 *Science* 35, 19–23. <https://doi.org/10.2135/cropsci1995.0011183X003500010004x>

827 Frank, A.B., Hofmann, L., 1989. Relationship among Grazing Management, Growing Degree-Days, and
828 Morphological Development for Native Grasses on the Northern Great Plains. *J. Range Manag.*
829 42, 199. <https://doi.org/10.2307/3899472>

830 Friesen, P.C., Cattani, D.J., 2017. Nitrogen use efficiency and productivity of first year switchgrass and
831 big bluestem from low to high soil nitrogen. *Biomass and Bioenergy* 107, 317–325.
832 <https://doi.org/10.1016/j.biombioe.2017.10.016>

833 Frischknecht, N.C., 1959. Effects of Presowing Vernalization on Survival and Development of Several
834 Grasses. *J. Range Manag.* 12, 280. <https://doi.org/10.2307/3894972>

835 Gall, H.J.F., 1947. Flowering of Smooth Brome Grass Under Certain Environmental Conditions.
836 *Botanical Gazette* 109, 59–71. <https://doi.org/10.1086/335456>

837 Gastal, F., Dawson, L.A., Thornton, B., 2010. Responses of plant traits of four grasses from contrasting
838 habitats to defoliation and N supply. *Nutr Cycl Agroecosyst* 88, 245–258.
839 <https://doi.org/10.1007/s10705-010-9352-x>

840 Gastal, F., Durand, J.-L., 2000. Effects of nitrogen and water supply on N and C fluxes and partitioning
841 in defoliated swards, in: *Grassland Ecophysiology and Grazing Ecology*. pp. 15–39.

842 Gastal, F., Lemaire, G., 2015. Defoliation, Shoot Plasticity, Sward Structure and Herbage Utilization in
843 Pasture: Review of the Underlying Ecophysiological Processes. *Agriculture* 5, 1146–1171.
844 <https://doi.org/10.3390/agriculture5041146>

845 Gate, P., 1995. *Ecophysiology du blé*. Tec & Doc-Lavoisier.

846 Glover, J.D., Reganold, J.P., Bell, L.W., Borevitz, J., Brummer, E.C., Buckler, E.S., Cox, C.M., Cox, T.S.,
847 Crews, T.E., Culman, S.W., DeHaan, L.R., Eriksson, D., Gill, B.S., Holland, J., Hu, F., Hulke, B.S.,
848 Ibrahim, A.M.H., Jackson, W., Jones, S.S., Murray, S.C., Paterson, A.H., Ploschuk, E., Sacks, E.J.,
849 Snapp, S., Tao, D., Tassel, D.L.V., Wade, L.J., Wyse, D.L., Xu, Y., 2010. Increased Food and
850 Ecosystem Security via Perennial Grains. *Science* 328, 1638–1639.
851 <https://doi.org/10.1126/science.1188761>

852 Halevy, A.H., 1989. *Handbook of Flowering*. CRC Press.

853 Hänsel, H., 1953. Vernalisation of Winter Rye by Negative Temperatures and the Influence of
854 Vernalisation upon the Lamina Length of the First and Second Leaf in Winter Rye, Spring Barley,
855 and Winter Barley. *Ann Bot* 17, 417–432. <https://doi.org/10.1093/oxfordjournals.aob.a083360>

856 Hastings, W.K., 1970. Monte Carlo sampling methods using Markov chains and their applications.
857 *Biometrika* 57, 97–109. <https://doi.org/10.1093/biomet/57.1.97>

858 Heide, O.M., 1994. Control of flowering and reproduction in temperate grasses. *New Phytologist* 128,
859 347–362. <https://doi.org/10.1111/j.1469-8137.1994.tb04019.x>

860 Heide, O.M., 1987. Photoperiodic control of flowering in *Dactylis glomerata*, a true short-long-day
861 plant. *Physiologia Plantarum* 70, 523–529. <https://doi.org/10.1111/j.1399-3054.1987.tb02853.x>

862 Heide, O.M., 1986. Primary and secondary induction requirements for flowering in *Alopecurus*
863 *pratensis*. *Physiologia Plantarum* 66, 251–256. <https://doi.org/10.1111/j.1399-3054.1986.tb02416.x>

864 Heide, O.M., 1984. Flowering requirements in *Bromus inermis*, a short-long-day plant. *Physiologia*
865 *Plantarum* 62, 59–64. <https://doi.org/10.1111/j.1399-3054.1984.tb05923.x>

866 Heide, O.M., 1980. Studies on flowering in *Poa pratensis* L. ecotypes and cultivars. *Meldinger fra*
867 *Norges Landbrukshogskole* 59.

868 Heide, O.M., Bush, M.G., Evans, L.T., 1987. Inhibitory and promotive effects of gibberellic acid on
869 floral initiation and development in *Poa pratensis* and *Bromus inermis*. *Physiologia Plantarum*
870 69, 342–350. <https://doi.org/10.1111/j.1399-3054.1987.tb04298.x>

871 Hess, M., Barralis, G., Bleiholder, H., Buhr, L., Eggers, T., Hack, H., Stauss, R., 1997. Use of the
872 extended BBCH scale—general for the descriptions of the growth stages of mono; and
873 dicotyledonous weed species. *Weed Research* 37, 433–441. <https://doi.org/10.1046/j.1365-3180.1997.d01-70.x>

874 Hunt, W.F., Halligan, G., 1981. Growth and Developmental Responses of Perennial Ryegrass Grown at
875 Constant Temperature. I. Influence of Light and Temperature on Growth and Net Assimilation.
876 *Functional Plant Biol.* 8, 181–190. <https://doi.org/10.1071/pp9810181>

877 Hunter, M.C., Sheaffer, C.C., Culman, S.W., Jungers, J.M., 2020. Effects of defoliation and row spacing
878 on intermediate wheatgrass i: Grain production. *Agronomy Journal*.
879 <https://doi.org/10.1002/agj2.20128>

880 Ivancic, K., Locatelli, A., Tracy, B., Picasso, V., *under review*. Kernza intermediate wheatgrass
881 (Thinopyrum intermedium) response to a range of vernalization conditions. *Can. J. Plant Sci.*

882 Jégo, G., Chantigny, M., Pattey, E., Bélanger, G., Rochette, P., Vanasse, A., Goyer, C., 2014. Improved
883 snow-cover model for multi-annual simulations with the STICS crop model under cold, humid
884 continental climates. *Agricultural and Forest Meteorology* 195–196, 38–51.
885 <https://doi.org/10.1016/j.agrformet.2014.05.002>

888 Jokela, V., Trevaskis, B., Seppänen, M.M., 2015. Genetic variation in the flowering and yield
889 formation of timothy (*Phleum pratense* L.) accessions after different photoperiod and
890 vernalization treatments. *Front. Plant Sci.* 6. <https://doi.org/10.3389/fpls.2015.00465>

891 Jungers, J.M., DeHaan, L.R., Betts, K.J., Sheaffer, C.C., Wyse, D.L., 2017. Intermediate Wheatgrass
892 Grain and Forage Yield Responses to Nitrogen Fertilization. *Agronomy Journal* 109, 462–472.
893 <https://doi.org/10.2134/agronj2016.07.0438>

894 Jungers, J.M., Frahm, C.S., Tautges, N.E., Ehlke, N.J., Wells, M.S., Wyse, D.L., Sheaffer, C.C., 2018.
895 Growth, development, and biomass partitioning of the perennial grain crop *Thinopyrum*
896 *intermedium*: Growth, development, and biomass partitioning of a perennial grain crop. *Annals*
897 *of Applied Biology*. <https://doi.org/10.1111/aab.12425>

898 Khan, M.A., Stace, C.A., 1999. Breeding relationships in the genus *Brachypodium* (Poaceae:
899 Pooideae). *Nordic Journal of Botany* 19, 257–269. <https://doi.org/10.1111/j.1756-1051.1999.tb01108.x>

900 Limin, A.E., Fowler, D.B., 2006. Low-temperature tolerance and genetic potential in wheat (*Triticum*
901 *aestivum* L.): response to photoperiod, vernalization, and plant development. *Planta* 224, 360–
902 366. <https://doi.org/10.1007/s00425-006-0219-y>

903 Loague, K., Green, R.E., 1991. Statistical and graphical methods for evaluating solute transport
904 models: Overview and application. *Journal of Contaminant Hydrology, Validation of Flow and*
905 *Transport Models for the Unsaturated Zone* 7, 51–73. [https://doi.org/10.1016/0169-7722\(91\)90038-3](https://doi.org/10.1016/0169-7722(91)90038-3)

906 Luo, Q., 2011. Temperature thresholds and crop production: a review. *Climatic Change* 109, 583–598.
907 <https://doi.org/10.1007/s10584-011-0028-6>

908 Mahfoozi, S., Limin, A.E., Hayes, P.M., Hucl, P., Fowler, D.B., 2000. Influence of photoperiod response
909 on the expression of cold hardiness in wheat and barley. *Can. J. Plant Sci.* 80, 721–724.
910 <https://doi.org/10.4141/P00-031>

911 Medina-Roldán, E., Bardgett, R.D., 2011. Plant and soil responses to defoliation: a comparative study
912 of grass species with contrasting life history strategies. *Plant Soil* 344, 377–388.
913 <https://doi.org/10.1007/s11104-011-0756-4>

914 Metropolis, N., Rosenbluth, A.W., Rosenbluth, M.N., Teller, A.H., Teller, E., 1953. Equation of State
915 Calculations by Fast Computing Machines. *J. Chem. Phys.* 21, 1087–1092.
916 <https://doi.org/10.1063/1.1699114>

917 Mitchell, R.B., Moore, K.J., Moser, L.E., Fritz, J.O., Redfearn, D.D., 1997. Predicting Developmental
918 Morphology in Switchgrass and Big Bluestem. *Agronomy Journal* 89, 827–832.
919 <https://doi.org/10.2134/agronj1997.00021962008900050018x>

920 Mitchell, R.B., Moser, L.E., Moore, K.J., Redfearn, D.D., 1998. Tiller Demographics and Leaf Area Index
921 of Four Perennial Pasture Grasses. *Agronomy Journal* 90, 47–53.
922 <https://doi.org/10.2134/agronj1998.00021962009000010009x>

923 Nelson, C.J., 2000. Shoot morphological plasticity of grasses: leaf growth vs. tillering. *Grassland*
924 *ecophysiology and grazing ecology* 101–126.

925 Palit, R., Bai, Y., Romo, J., Coulman, B., Pierre, R.S., 2014. Variations in vernalization requirements
926 among ecotypes of *Festuca hallii*. *Grass and Forage Science* 70, 353–364.
927 <https://doi.org/10.1111/gfs.12101>

928 Parthasarathi, T., Velu, G., Jeyakumar, P., 2013. Impact of Crop Heat Units on Growth and
929 Developmental Physiology of Future Crop Production: A Review 2, 9

930 Peacock, J.M., 1976. Temperature and Leaf Growth in Four Grass Species. *Journal of Applied Ecology*
931 13, 225–232. <https://doi.org/10.2307/2401942>

932 Peel, M.C., Finlayson, B.L., McMahon, T.A., 2007. Updated world map of the Köppen-Geiger climate
933 classification. *Hydrology and Earth System Sciences Discussions* 4, 439–473.

934 Poorter, H., Remkes, C., 1990. Leaf area ratio and net assimilation rate of 24 wild species differing in
935 relative growth rate. *Oecologia* 83, 553–559. <https://doi.org/10.1007/BF00317209>

936 Porter, J.R., Gawith, M., 1999. Temperatures and the growth and development of wheat: a review.
937 *European Journal of Agronomy* 10, 23–36. [https://doi.org/10.1016/S1161-0301\(98\)00047-1](https://doi.org/10.1016/S1161-0301(98)00047-1)

940 Ritchie, J.T., 1991. Wheat Phasic Development, in: Modeling Plant and Soil Systems. John Wiley &
941 Sons, Ltd, pp. 31–54. <https://doi.org/10.2134/agronmonogr31.c3>

942 Ryan, M.R., Crews, T.E., Culman, S.W., DeHaan, L.R., Hayes, R.C., Jungers, J.M., Bakker, M.G., 2018.
943 Managing for Multifunctionality in Perennial Grain Crops. *BioScience* 68, 294–304.

944 Ryser, P., Lambers, H., 1995. Root and leaf attributes accounting for the performance of fast- and
945 slow-growing grasses at different nutrient supply. *Plant Soil* 170, 251–265.
946 <https://doi.org/10.1007/BF00010478>

947 Sanderson, M.A., West, C.P., Moore, K.J., Stroup, J., Moravec, J., 1997. Comparison of Morphological
948 Development Indexes for Switchgrass and Bermudagrass. *Crop Science* 37, 871–878.
949 <https://doi.org/10.2135/cropsci1997.0011183X003700030029x>

950 Sellers, W.D., 1965. Physical climatology, University of Chicago. ed.

951 Seppänen, M.M., Korhonen, P., Jokela, V., Isolanti, M., Virkajärvi, P., 2013. The role of vernalization in
952 freezing tolerance and tiller composition of forage grasses. The role of grasslands in a green
953 future: threats and perspectives in less favoured areas. Proceedings of the 17th Symposium of
954 the European Grassland Federation, Akureyri, Iceland, 23-26 June 2013 297–299.

955 Shipley, B., 2006. Net assimilation rate, specific leaf area and leaf mass ratio: which is most closely
956 correlated with relative growth rate? A meta-analysis. *Functional Ecology* 20, 565–574.
957 <https://doi.org/10.1111/j.1365-2435.2006.01135.x>

958 Simon, J.C., Lemaire, G., 1987. Tillering and leaf area index in grasses in the vegetative phase. *Grass*
959 *and Forage Science* 42, 373–380. <https://doi.org/10.1111/j.1365-2494.1987.tb02127.x>

960 Sprunger, C.D., Culman, S.W., Robertson, G.P., Snapp, S.S., 2018. How Does Nitrogen and Perenniality
961 Influence Belowground Biomass and Nitrogen Use Efficiency in Small Grain Cereals? *Crop*
962 *Science* 0, 0. <https://doi.org/10.2135/cropsci2018.02.0123>

963 Tautges, N.E., Jungers, J.M., DeHaan, L.R., Wyse, D.L., Sheaffer, C.C., 2018. Maintaining grain yields of
964 the perennial cereal intermediate wheatgrass in monoculture v. bi-culture with alfalfa in the
965 Upper Midwestern USA. *The Journal of Agricultural Science* 1–16.
966 <https://doi.org/10.1017/S0021859618000680>

967 Ter Braak, C.J.F., 2006. A Markov Chain Monte Carlo version of the genetic algorithm Differential
968 Evolution: easy Bayesian computing for real parameter spaces. *Stat Comput* 16, 239–249.
969 <https://doi.org/10.1007/s11222-006-8769-1>

970 Trione, E.J., Metzger, R.J., 1970. Wheat and Barley Vernalization in a Precise Temperature Gradient1.
971 *Crop Science* 10, 390–392. <https://doi.org/10.2135/cropsci1970.0011183X001000040023x>

972 Vrugt, J.A., 2016. Markov chain Monte Carlo simulation using the DREAM software package: Theory,
973 concepts, and MATLAB implementation. *Environmental Modelling & Software* 75, 273–316.
974 <https://doi.org/10.1016/j.envsoft.2015.08.013>

975 Vrugt, J.A., Gupta, H.V., Bouten, W., Sorooshian, S., 2003. A Shuffled Complex Evolution Metropolis
976 algorithm for optimization and uncertainty assessment of hydrologic model parameters. *Water*
977 *Resources Research* 39. <https://doi.org/10.1029/2002WR001642>

978 Vrugt J.A., ter Braak C.J.F., Diks C.G.H., Robinson B.A., Hyman J.M., Higdon D., 2009. Accelerating
979 Markov Chain Monte Carlo Simulation by Differential Evolution with Self-Adaptive Randomized
980 Subspace Sampling. *International Journal of Nonlinear Sciences and Numerical Simulation* 10,
981 273–290. <https://doi.org/10.1515/IJNSNS.2009.10.3.273>

982 Wallach, D., Makowski, D., Jones, J.W. (Eds.), 2006. Evaluation, analysis, parameterization and
983 applications, in: Working with Dynamic Crop Models. Academic Press.

984 Wang, E., Martre, P., Zhao, Z., Ewert, F., Maiorano, A., Rötter, R.P., Kimball, B.A., Ottman, M.J., Wall,
985 G.W., White, J.W., Reynolds, M.P., Alderman, P.D., Aggarwal, P.K., Anothai, J., Basso, B.,
986 Biernath, C., Cammarano, D., Challinor, A.J., De Sanctis, G., Doltra, J., Dumont, B., Fereres, E.,
987 Garcia-Vila, M., Gayler, S., Hoogenboom, G., Hunt, L.A., Izaurralde, R.C., Jabloun, M., Jones, C.D.,
988 Kersebaum, K.C., Koehler, A.-K., Liu, L., Müller, C., Naresh Kumar, S., Nendel, C., O’Leary, G.,
989 Olesen, J.E., Palosuo, T., Priesack, E., Eyshi Rezaei, E., Ripoche, D., Ruane, A.C., Semenov, M.A.,
990 Shcherbak, I., Stöckle, C., Stratonovitch, P., Streck, T., Supit, I., Tao, F., Thorburn, P., Waha, K.,
991 Wallach, D., Wang, Z., Wolf, J., Zhu, Y., Asseng, S., 2017. The uncertainty of crop yield projections

992 is reduced by improved temperature response functions. Nat. Plants 3.
993 <https://doi.org/10.1038/nplants.2017.102>
994
995
996
997
998